Submitted to Nuclear Physics A FSU-SCRI-96-08

The Okamoto-Nolen-Schiffer anomaly without ρ-ω mixing

F. Cardarelli
Department of Physics and Supercomputer Computations Research Institute, Florida State University, Tallahassee, FL 32306

J. Piekarewicz
Supercomputer Computations Research Institute, Florida State University, Tallahassee, FL 32306

(January 4, 2014)

arXiv:nucl-th/9602010v2 30 May 1996

Abstract

We examine the effect of isospin-violating meson-nucleon coupling constants and of π-η mixing on the binding-energy differences of mirror nuclei in a model that possesses no contribution from ρ-ω mixing. The ^{3}He-^{3}H binding-energy difference is computed in a nonrelativistic approach using a realistic wave function. We find the ^{3}He-^{3}H binding-energy difference very sensitive to the short-distance behavior of the nucleon-nucleon potential. We conclude that for the typically hard Bonn form factors such models can not account for the observed binding-energy difference in the three-nucleon system. For the medium-mass region (A=15–41) the binding-energy differences of mirror nuclei are computed using a relativistic mean-field approximation to the Walecka model. We obtain large binding-energy differences—of the order of several hundred keV—arising from the pseudoscalar sector. Two effects are primarily responsible for this new finding: a) the inclusion of isospin breaking in the pion-nucleon coupling constant, and b) the in-medium enhancement of the small components of the bound-state wave functions. We look for off-shell ambiguities in these results and find them to be large.

PACS number(s): 21.10.Dr, 24.10.Jv, 13.75.Gx

Typeset using REVTEX

I. INTRODUCTION

Some of our most fundamental ideas about charge-symmetry-breaking (CSB) phenomena in nuclear physics [1,2] are currently being revisited. To a large extent this revision has been prompted by the suggestion of Goldman, Henderson, and Thomas of a suppressed contribution from ρ-ω mixing to the CSB component of the nucleon-nucleon (NN) interaction at small momentum transfers [3]. Since then, many calculations, using a variety of theoretical approaches, have confirmed this suppression [4,5,6,7,8,9]. Although the issue continues to be controversial [10,11], the search for alternate CSB mechanisms has already started. Indeed, in a recent publication we have proposed isospin breaking in the meson-nucleon vertices as an additional source of isospin violation [12]. We have used isospin breaking in the pion-nucleon coupling constant [13] to account for the large isospin violation in the pion-nucleon system reported recently by Gibbs, Ai, and Kaufmann [14]. Moreover, we have studied the impact of isospin violation in the vector-meson–nucleon coupling constants on the difference between the neutron and proton analyzing powers (ΔA) measured in elastic $\vec{n}$-$\vec{p}$ scattering [15]. We have concluded that the magnitude of the resulting class IV CSB potential was consistent with that phenomenologically required by the experiment [12].

However, other CSB observables, such as the scattering-length differences of the pp and nn systems [16], and the binding-energy differences of mirror nuclei—the Okamoto-Nolen-Schiffer (ONS) anomaly [17,18]—are particularly insensitive to the class IV component of the CSB potential. Rather, these observables are driven by the class III component. Indeed, several authors [19,20,21] have observed that the class III component of the CSB potential—generated from "on-shell" ρ-ω mixing—dominates the binding-energy discrepancy of mirror nuclei and could explain most of the ONS anomaly [2].

Motivated by the recent developments, we propose to study the ONS anomaly in a model which possesses no contribution from ρ-ω mixing; in our model, the resulting CSB potential is generated exclusively from π-η mixing and from isospin violation in the meson-nucleon coupling constants. To compute the ^{3}He-^{3}H binding-energy difference we employ a realistic three-body wave function obtained from the variational analysis of Ref. [22] using the Reid-soft core potential. To study the ONS anomaly in the A=15–41 region we use a relativistic mean-field approximation to the Walecka model [23]. Although the Walecka model has been used recently to compute binding-energy differences in mirror nuclei [24,25,26], these studies have been limited to the vector sector: Coulomb corrections plus on-shell ρ-ω mixing. However, since these contributions are dominated by the timelike part of the vector vertex (γ^0) they are not particularly sensitive to relativistic effects. In contrast, one expects important relativistic corrections in the pseudoscalar sector because of the structure of the (γ^5) vertex. Examining the role of relativistic effects and of isospin violation in the meson-nucleon coupling constants are two of the major components of the present investigation.

Our paper has been organized as follows. In Sec. II we introduce the CSB potentials derived from meson mixing and from isospin violation in the meson-nucleon coupling constants. There, we review some of the ideas germane to our model. Sec. III is reserved to the analysis of the ONS anomaly in the three-nucleon system with special emphasis placed on the sensitivity of our results to the choice of hadronic form factors. Binding-energy differences of A=15–41 mirror nuclei are computed in Sec. IV using various off-shell extrapolations of the NN potential. Finally, we present our conclusions in Sec. V.

II. CHARGE-SYMMETRY-BREAKING POTENTIALS

A. Vector-meson sector

The CSB potentials which arise from isospin violation in the vector-meson–nucleon vertices and from ρ-ω mixing are given, respectively, by [1,2,12]

$$\widehat{V}^{\omega}_{\rm CSB} = V^{\omega}_{\rm CSB}(Q^2)\Big[\Gamma^{\mu}(1)\gamma_{\mu}(2)\tau_z(1) + \gamma^{\mu}(1)\Gamma_{\mu}(2)\tau_z(2)\Big] \ , \tag{1a}$$

$$\widehat{V}^{\rho}_{\rm CSB} = V^{\rho}_{\rm CSB}(Q^2)\Big[\Gamma^{\mu}(1)\gamma_{\mu}(2)\tau_z(2) + \gamma^{\mu}(1)\Gamma_{\mu}(2)\tau_z(1)\Big] + V'^{\rho}_{\rm CSB}(Q^2)\left[\Gamma^{\mu}(1)\Gamma_{\mu}(2)\Big(\tau_z(1)+\tau_z(2)\Big)\right] \ , \tag{1b}$$

$$\widehat{V}^{\rho\omega}_{\rm CSB} = V^{\rho\omega}_{\rm CSB}(Q^2)\left[\gamma^{\mu}(1)\gamma_{\mu}(2)\Big(\tau_z(1)+\tau_z(2)\Big)\right] + V'^{\rho\omega}_{\rm CSB}(Q^2)\Big[\Gamma^{\mu}(1)\gamma_{\mu}(2)\tau_z(1) + \gamma^{\mu}(1)\Gamma_{\mu}(2)\tau_z(2)\Big] \ . \tag{1c}$$

where $Q^2 \equiv -q_{\mu}^2$ is the negative of the four-momentum transfer, $\Gamma^{\mu} \equiv i\sigma^{\mu\nu}(p'-p)_{\nu}/2M$, and we have defined

$$V^{\omega}_{\rm CSB}(Q^2) \equiv \frac{g^2_{NN\omega}}{Q^2+m^2_{\omega}} f^{\omega}_1 \ , \tag{2a}$$

$$V^{\rho}_{\rm CSB}(Q^2) \equiv \frac{g^2_{NN\rho}}{Q^2+m^2_{\rho}} f^{\rho}_0 \ , \tag{2b}$$

$$V'^{\rho}_{\rm CSB}(Q^2) \equiv \frac{g_{NN\rho} f_{NN\rho}}{Q^2+m^2_{\rho}} f^{\rho}_0 \ , \tag{2c}$$

$$V^{\rho\omega}_{\rm CSB}(Q^2) \equiv -\frac{g_{NN\rho} g_{NN\omega}}{(Q^2+m^2_{\rho})(Q^2+m^2_{\omega})} \langle\rho|H|\omega\rangle \ , \tag{2d}$$

$$V'^{\rho\omega}_{\rm CSB}(Q^2) \equiv -\frac{f_{NN\rho} g_{NN\omega}}{(Q^2+m^2_{\rho})(Q^2+m^2_{\omega})} \langle\rho|H|\omega\rangle \ . \tag{2e}$$

Note that $g_{NN\omega}$, $g_{NN\rho}$, and $f_{NN\rho}$, are the isospin-conserving meson-nucleon coupling constants extracted from fits to two nucleon data and displayed in Table I using the Bonn B potential model [27]. Charge-symmetry breaking in the potentials is characterized by the appearance of three isospin-violating parameters: f^{ω}_1, f^{ρ}_0, and $\langle\rho|H|\omega\rangle$; an isovector-tensor $NN\omega$ coupling constant, an isoscalar-tensor $NN\rho$ coupling constant, and the ρ-ω mixing amplitude, respectively.

Our model is inspired by the notion of vector-meson dominance (VMD), so that the vector mesons couple to the appropriate isospin components of a conserved electromagnetic current. In models of this kind the ρ-ω mixing amplitude necessarily vanishes at $Q^2 = 0$ [4,8]. Moreover, our VMD assumption places important constraints on the form of the isospin-violating vector-meson–nucleon vertex at $Q^2 = 0$. Specifically, isospin breaking can occur only in the tensor part of the vertex; the vector coupling is protected by gauge invariance [12,28,29]. Thus, gauge invariance precludes the appearance of a class III—vector-vector—component in the CSB potential generated from vector-meson exchange. For the analysis of ΔA this fact is of no consequence, as class III CSB potentials do not contribute to np observables. Indeed, the class IV contribution from ω-meson exchange is able to fill

the role demanded by data; recall that this term is identical in structure and comparable in size to the one generated from on-shell ρ-ω mixing [12]. However, for observables in which the vector-vector component of $\widehat{V}^{\rho\omega}_{\rm CSB}$ was believed to be dominant—such as in the case of the ONS anomaly [19,20,21]—the absence of the corresponding term from $\widehat{V}^{\omega}_{\rm CSB}$ and $\widehat{V}^{\rho}_{\rm CSB}$ could have important phenomenological consequences. This conclusion is unavoidable: it follows directly from gauge invariance; gauge invariance forces the isospin-violating vector coupling and the ρ-ω mixing amplitude to vanish at $Q^2 = 0$.

B. Pseudoscalar-meson sector

The CSB potential which emerges from isospin violations in the pseudoscalar-meson sector is given by,

$$\widehat{V}^{(5)}_{\rm CSB} = V^{(5)}_{\rm CSB}(Q^2)\gamma^5(1)\gamma^5(2)\Big[\tau_z(1)+\tau_z(2)\Big] \,, \tag{3a}$$

$$V^{(5)}_{\rm CSB}(Q^2) = V^{\pi}_{\rm CSB}(Q^2) + V^{\pi\eta}_{\rm CSB}(Q^2) \,, \tag{3b}$$

with $V^{(5)}_{\rm CSB}$ made out of contributions arising from isospin violation in the pion-nucleon vertex and from π-η mixing [12], respectively,

$$V^{\pi}_{\rm CSB}(Q^2) \equiv \frac{g^2_{NN\pi}}{Q^2+m^2_\pi} g^\pi_0 \,, \tag{4a}$$

$$V^{\pi\eta}_{\rm CSB}(Q^2) \equiv -\frac{g_{NN\pi}g_{NN\eta}}{(Q^2+m^2_\pi)(Q^2+m^2_\eta)}\langle\pi|H|\eta\rangle \,. \tag{4b}$$

The isospin-conserving pion-nucleon coupling constant $g_{NN\pi}$ is given by the Bonn B potential value listed in Table I. For the $NN\eta$ coupling constant we have decided to use a value extracted from SU(3)-flavor symmetry [30], rather than the Bonn-potential value of $g^2_{NN\eta}/4\pi = 2.25$. Indeed, it is believed that the Bonn potential overestimates the coupling; a recent analysis based on η-photoproduction data suggests values as low as $g^2_{NN\eta}/4\pi \lesssim 0.5$ [31] (see also Ref. [32]). For the ηN cutoff parameter we have simply assumed: $\Lambda_{NN\eta} = \Lambda_{NN\pi}$. The two parameters driving the CSB potential are the isospin-violating pion-nucleon coupling constant (g^π_0) and the π-η mixing amplitude ($\langle\pi|H|\eta\rangle$). CSB potentials derived from π-η mixing have been included in previous nonrelativistic analyses of the ONS anomaly [19,21,30]. However, to our knowledge, CSB potentials arising from isospin violation in the meson-nucleon coupling constants have never been incorporated into these analyses, and only recently have they been used to study isospin violations in low-energy pion-nucleon scattering [13].

III. BINDING-ENERGY DIFFERENCE IN THE A=3 SYSTEM

In this section we examine the effect of π-η mixing and of isospin-violating meson-nucleon coupling constants on the ^{3}He-^{3}H binding-energy difference. Experimentally, this difference is very precisely known and has the value of 764 keV. A nearly model-independent method for estimating the electromagnetic contribution to the binding-energy difference has

already been developed [20,33]; ambiguities remain, however, on how to separate the meson-exchange-current component from the experimental charge form factors. These estimates suggest an electromagnetic contribution to the binding-energy of $693 \pm 19 \pm 5$ keV, leaving $71 \pm 19 \pm 5$ keV to be explained by charge-symmetry-breaking effects [2,20]. Note that a very similar result has been obtained recently by Ishikawa and Sasakawa using a different method [21]. These authors have also computed the contribution to the binding-energy difference arising from (on-shell) ρ-ω mixing and from π-η mixing, with the former playing the dominant role. Our model possesses no contribution from ρ-ω mixing. Hence, we would like to investigate the possible role of alternate CSB mechanisms in accounting for the non-electromagnetic contribution to the ^{3}He-^{3}H binding-energy difference:

$$\Delta E = \langle {}^3He|V_{pp}|{}^3He\rangle - \langle {}^3H|V_{nn}|{}^3H\rangle \equiv -\langle {}^3He|\Delta V|{}^3He\rangle \ . \tag{5}$$

We shall compute the ^{3}He-^{3}H binding-energy difference using the realistic three-body wave function obtained from the variational analysis of Numberg, Prosperi, and Pace [22]. These authors have written the nuclear Hamiltonian

$$H = \frac{1}{2M}(\mathbf{p}_a^2 + 3\mathbf{p}_b^2) + \sum_{\substack{i,j=1 \\ (i<j)}}^{3} V_{ij} \ , \tag{6}$$

in terms of the two intrinsic coordinates

$$\mathbf{a} = \sqrt{\frac{1}{2}}(\mathbf{r}_1 - \mathbf{r}_2) \ ; \quad \mathbf{b} = \sqrt{\frac{1}{2}}(2\mathbf{r}_3 - \mathbf{r}_1 - \mathbf{r}_2) \ , \tag{7}$$

and their corresponding conjugate momenta. Note that the indices 1 and 2 are reserved for the identical particles in the system; this is particularly convenient for the perturbative estimate of the ^{3}He-^{3}H binding-energy shift. The basic dynamical input is contained in the two-nucleon interaction (V_{ij}) which was chosen to be the Reid soft-core potential [34]. Matrix elements of the Hamiltonian were computed using a truncated basis of 820 harmonic-oscillator states and the ground-state wave function was obtained from direct matrix diagonalization. This wave function provides a satisfactory description of the charge form factors of ^{3}He and ^{3}H in the low-momentum-transfer region [22,35]. Moreover, a perturbative estimate of the Coulomb shift in ^{3}He yields 672 keV—a value consistent with that reported in Refs. [20,21].

For simplicity, the binding energy difference will be evaluated with the dominant $^1S_0$ component of the trinucleon wave function. Note that for this case it is sufficient to evaluate the $^1S_0$ component of the CSB potential:

$$\Delta V \equiv V_{nn}({}^1S_0) - V_{pp}({}^1S_0) \ . \tag{8}$$

The singlet CSB component of the NN potential is obtained by performing a nonrelativistic reduction of the various Lorentz structures given in Eqs. (1,3) and by evaluating the meson propagators in the static limit [1,36]. We obtain ($f_1^\rho \equiv f_{NN\rho}/g_{NN\rho}$)

$$\Delta V^{\pi\eta}(\mathbf{q}) = g_{NN\pi}g_{NN\eta}\langle\pi|H|\eta\rangle \frac{\mathbf{q}^2/M^2}{(\mathbf{q}^2 + m_\pi^2)(\mathbf{q}^2 + m_\eta^2)} \ , \tag{9a}$$

$$\Delta V^{\pi}(\mathbf{q}) = -g^2_{NN\pi} g^{\pi}_0 \frac{\mathbf{q}^2/M^2}{\mathbf{q}^2 + m^2_{\pi}} \; , \tag{9b}$$

$$\Delta V^{\rho}(\mathbf{q}) = -g^2_{NN\rho} (1 + 2f^{\rho}_1) f^{\rho}_0 \frac{\mathbf{q}^2/M^2}{\mathbf{q}^2 + m^2_{\rho}} \; , \tag{9c}$$

$$\Delta V^{\omega}(\mathbf{q}) = -g^2_{NN\omega} f^{\omega}_1 \frac{\mathbf{q}^2/M^2}{\mathbf{q}^2 + m^2_{\omega}} \; . \tag{9d}$$

Note the appearance of the "relativistic-correction" factor $\mathbf{q}^2/M^2$. This factor emerges from the allowed Lorentz structures present in the CSB potentials. Recall that—in contrast to previous analyses based on on-shell ρ-ω mixing—no Lorentz vector structure $[\gamma^{\mu}(1)\gamma_{\mu}(2)]$ is allowed in our model. For the π-η mixing amplitude we have used the accepted value of $\langle \pi | H | \eta \rangle = -4200$ MeV^2 [30]. For the isospin-violating meson-nucleon parameter we have adopted the nonrelativistic quark-model estimate of Refs. [12]:

$$g^{\pi}_0 = \frac{3}{10} \frac{\Delta m}{m} \approx 0.004 \; , \tag{10a}$$

$$f^{\rho}_0 = \frac{3}{2} \frac{\Delta m}{m} \approx 0.020 \; , \tag{10b}$$

$$f^{\omega}_1 = \frac{5}{6} \frac{\Delta m}{m} \approx 0.011 \; , \tag{10c}$$

where $m = 313$ MeV is the average constituent quark mass and $\Delta m = 4.1$ MeV is the down-up quark mass difference [37]. Although these values are model dependent, they are insensitive to the spatial component of the nucleon wave function; they follow directly from its spin and flavor content. Moreover, the value of g^{π}_0 is compatible with other estimates available in the literature [2] and, in particular, with the recent value reported by Henley and Meissner from QCD sum rules [38].

To facilitate the interpretation of our results it is convenient to transform the above expressions into configuration space:

$$\Delta V^{\pi\eta}(r) = \frac{g_{NN\pi} g_{NN\eta}}{4\pi} \frac{\langle \pi | H | \eta \rangle}{m^2_{\eta} - m^2_{\pi}} \left[\left(\frac{m_{\eta}}{M} \right)^2 \frac{e^{-m_{\eta} r}}{r} - \left(\frac{m_{\pi}}{M} \right)^2 \frac{e^{-m_{\pi} r}}{r} \right] \; , \tag{11a}$$

$$\Delta V^{\pi}(r) = \frac{g^2_{NN\pi}}{4\pi} g^{\pi}_0 \left[\left(\frac{m_{\pi}}{M} \right)^2 \frac{e^{-m_{\pi} r}}{r} - \frac{\delta(r)}{M^2 r^2} \right] \; , \tag{11b}$$

$$\Delta V^{\rho}(r) = \frac{g^2_{NN\rho}}{4\pi} (1 + 2f^{\rho}_1) f^{\rho}_0 \left[\left(\frac{m_{\rho}}{M} \right)^2 \frac{e^{-m_{\rho} r}}{r} - \frac{\delta(r)}{M^2 r^2} \right] \; , \tag{11c}$$

$$\Delta V^{\omega}(r) = \frac{g^2_{NN\omega}}{4\pi} f^{\omega}_1 \left[\left(\frac{m_{\omega}}{M} \right)^2 \frac{e^{-m_{\omega} r}}{r} - \frac{\delta(r)}{M^2 r^2} \right] \; . \tag{11d}$$

Note that in configuration space the ^{3}He-^{3}H binding-energy difference emerges from a simple overlap between the singlet component of the wave function $[R(a)]$ and the CSB potential

$$\Delta E = -\int_0^{\infty} a^2 da |R(a)|^2 \Delta V(\sqrt{2}a) \equiv \int_0^{\infty} I(a) da \; . \tag{12}$$

We will refer to these estimates as the point-coupling results, as hadronic form factor have yet to be introduced. We note, as a consequence of the relativistic factor $\mathbf{q}^2/M^2$, the appearance

of a contact term [$\delta(r)$] in all single-meson exchanges (the contact term is absent from the π-η mixing potential because of the additional meson propagator). For realistic wave functions—such as the one used here—the contact term does not contribute to the overlap as a result of the repulsive short-range correlations. Thus, we conclude that all single-meson-exchange potentials generate a repulsive ΔV, namely, a CSB potential that is attractive(repulsive) in the $pp(nn)$ channel—in contrast to the experimental observation. Note that this conclusion depends exclusively on the sign of the isospin-violating meson-nucleon coupling constants; recall that in our model these constants are all positive as a result of the up quark being lighter than the down quark.

This conclusion could change dramatically upon the inclusion of hadronic form factors. With form factors the contact term gets smeared over a distance of the order of Λ^{-1} (with Λ being the cutoff parameter) and could contribute to the overlap if this distance becomes larger than the size of the repulsive core. Most of our knowledge about hadronic form factor comes from phenomenological fits to a large body of two-nucleon data [27]. These fits reveal hadronic form factors that are typically harder ($\Lambda \gtrsim 1.5$ GeV) than the corresponding ones extracted from electron-nucleon scattering experiments ($\Lambda \simeq 0.8$ GeV). However, the subject of hadronic form factors is highly controversial. Indeed, (model-dependent) analyses of deep-inelastic-scattering (DIS) experiments suggest that the $NN\pi$ form factor is considerably softer than $\Lambda_{NN\pi} \sim 1.5$ GeV [39,40,41]. Moreover, Holinde and Thomas have shown recently that it is possible to obtain an adequate description of two-nucleon data with the softer pion-nucleon form factor ($\Lambda_{NN\pi} \simeq 0.8$ GeV) suggested by the DIS analyses [42]. These authors have also shown that the $NN\rho$ form factor can also be made softer—but no softer than $\Lambda_{NN\rho} \simeq 1.2$ GeV—without compromising the fit. Hence, we find it instructive to do the calculation of the ^{3}He-^{3}H binding-energy shift using, both, the hard form factors of Table I as well as the softer ones suggested by the analyses of Refs. [39,40,41,42]. In the latter case we fix, for simplicity, both pseudoscalar cutoff parameters at $\Lambda_{NN\pi(\eta)} = 0.8$ GeV and both vector cutoff parameters at $\Lambda_{NN\rho(\omega)} = 1.3$ GeV. We incorporate hadronic form factors into the calculation by modifying the point meson-nucleon coupling in the following way [27]:

$$g_{NN\pi(\eta)} \rightarrow g_{NN\pi(\eta)}(\mathbf{q}^2) = g_{NN\pi(\eta)}(1 + \mathbf{q}^2/\Lambda^2_{\pi(\eta)})^{-1} \,, \tag{13a}$$

$$g_{NN\rho(\omega)} \rightarrow g_{NN\rho(\omega)}(\mathbf{q}^2) = g_{NN\rho(\omega)}(1 + \mathbf{q}^2/\Lambda^2_{\rho(\omega)})^{-2} \,. \tag{13b}$$

In Table II we report the contribution to the ^{3}He-^{3}H binding-energy difference arising from π-η mixing, $\pi-$, $\rho-$, and $\omega-$meson exchange, respectively. For comparison, we have also included the contribution arising from ρ-ω mixing, with the mixing amplitude fixed at its on-shell value: $\langle\rho|H|\omega\rangle = -4520$ MeV^2 [20]. The first column of numbers displays the results in the point-coupling limit. As suggested, all single meson-exchange potentials give rise to a negative binding-energy shift; only π-η mixing leads to a positive—albeit very small—contribution. The binding energy-shifts computed with the Bonn B hadronic form factors are reported in Table II under the heading of hard form factors. Evidently, the binding-energy shift is very sensitive to the short-distance behavior of the potential; the inclusion of form factors results in a 40% reduction relative to the point-coupling estimate. This reduction is best appreciated by plotting the integrand from which ΔE is obtained, that is $I(a)$ in Eq. (12). In Fig. 1 we display the contribution from one-pion exchange to $I(a)$; its contribution to ΔE for each estimate, which is the area under the curve, appears in parentheses next to its label. The solid line represents the point-coupling result. In this case

the contact term does not contribute and the integrand is negative-definite over the whole region. As the (hard) Bonn form factor is introduced (dashed line) the smeared contact term dominates the short-distance region and cancels some of the negative contribution arising from the long-range term. It is then clear that for a sufficiently soft form factor the node in the potential—arising from the competition between the short- and long-range pieces—could be moved to a large enough distance as to make the integral positive; this is precisely what is observed when the softer form factor is introduced (dot-dashed line). The complete set of numbers with soft form factors has been collected on Table II. For completeness we have also displayed in Fig. 2 the corresponding integrand for the omega meson. The same features are evident. In the present case, however, the integral is negative in all three cases because the vector form factor remains fairly hard. Nevertheless, we should mention that even for the case of (perhaps) unrealistically soft form factors, namely $\Lambda_{NN\pi(\eta)} = 0.6$ GeV and $\Lambda_{NN\rho(\omega)} = 0.85$ GeV, our model can only account for +40 keV of the ^{3}He-^{3}H binding-energy difference; a result that is still one standard deviation away from the experimental value.

In conclusion, we have shown that an analysis based on π-η mixing and on isospin-violating meson-nucleon coupling constants—but one without ρ-ω mixing—can not describe the ^{3}He-^{3}H binding-energy difference. However, we have established that this finding is extremely sensitive to the least understood feature of the NN potential, namely, its short-distance structure. Thus, it is difficult to draw any definite conclusion until an accurate determination of the cutoff parameters in the meson-nucleon form factors is made—a very difficult task indeed.

IV. BINDING-ENERGY DIFFERENCES IN A=15–41 MIRROR NUCLEI

In this section we examine the effect of meson mixing and of isospin violation in the meson-nucleon coupling constants on the binding-energy differences of medium-mass mirror nuclei using a relativistic mean-field approximation to the Walecka model [23]. The Walecka model is a renormalizable strong-coupling field theory of nucleons interacting via the exchange of scalar and vector mesons. One of the great virtues of the model is its simplicity. Indeed, already at the mean-field level the Walecka model rivals some of the best available nonrelativistic calculations and provides a unified description of various nuclear properties, such as nuclear saturation, the spin-orbit force, and the density dependence of the nuclear interaction. The mean-field approximation is characterized by the existence of large Lorentz scalar and vector components that are responsible for a substantial in-medium enhancement of the small (lower) components of the single-particle wave functions; the so-called $M^\star$ effect.

A. Vector-meson sector

In our model ρ-ω mixing can not contribute to the ONS anomaly, at least at $Q^2 = 0$. Yet, a calculation of binding-energy shifts using the on-shell value for the ρ-ω mixing amplitude is still useful, as it provides a baseline against which alternate CSB mechanisms can be tested. Thus, we start this section by computing the impact of the dominant class III vector-vector component of $\widehat{V}^{\rho\omega}_{\rm CSB}$ to the ONS anomaly. The purpose of this exercise is to establish the size

of the phenomenological gap that will have to be filled by the alternate CSB mechanisms. Note that we will not report the contribution to the binding-energy differences arising from the tensor-vector and tensor-tensor terms in Eq. 1; for spin-saturated nuclei their numerical impact is small (typically less than 10%).

We compute the single-particle spectrum in a relativistic mean-field approximation to the Walecka model [23] and incorporate CSB corrections in the Hartree-Fock approximation, i.e.,

$$\Delta E_\alpha^{(0)} \equiv \Delta E_\alpha^H + \Delta E_\alpha^F \ , \tag{14}$$

where

$$\Delta E_\alpha^H = +4 \sum_\beta^{\rm occ} \int \frac{d\mathbf{q}}{(2\pi)^3} V_{\rm CSB}^{\rho\omega}(\mathbf{q}) \ \rho_{\alpha\alpha}^{(0)\star}(\mathbf{q}) \rho_{\beta\beta}^{(0)}(\mathbf{q}) \ , \tag{15a}$$

$$\Delta E_\alpha^F = -4 \sum_\beta^{\rm occ} \int \frac{d\mathbf{q}}{(2\pi)^3} V_{\rm CSB}^{\rho\omega}(\mathbf{q}) \ \left| \rho_{\beta\alpha}^{(0)}(\mathbf{q}) \right|^2 \ . \tag{15b}$$

Note that the factor of four appearing in the above expressions emerges from the characteristic class III isospin factor $\Big[\tau_z(1) + \tau_z(2)\Big]$. In Eq. (15) the sum runs over occupied orbitals in the Fermi sea, and we have introduced the Fourier transform of the off-diagonal timelike-vector density

$$\rho_{\beta\alpha}^{(0)}(\mathbf{q}) = \int d\mathbf{x} \, \overline{\mathcal{U}}_\beta(\mathbf{x}) \gamma^0 e^{-i\mathbf{q}\cdot\mathbf{x}} \, \mathcal{U}_\alpha(\mathbf{x}) \ . \tag{16}$$

Several remarks are in order. First, we have ignored the contribution from the Dirac sea (negative-energy states) in the evaluation of the single-particle spectrum as well as in the CSB corrections to the energies. Second, for spherically symmetric nuclei only the timelike part $[\gamma^0(1)\gamma^0(2)]$ of the potential contributes to the Hartree term; for static sources and fields, current conservation prohibits the appearance of a three-vector current [23]. Thus, as far as the Hartree term is concerned, the CSB potential generated from ρ-ω mixing behaves as a short-range Coulomb potential. Third, even though the spacelike-part $[\boldsymbol{\gamma}(1)\cdot\boldsymbol{\gamma}(2)]$ of the potential contributes to the Fock term, it is of little numerical significance and has been neglected. Finally, we suppress vector-meson production by ignoring retardation effects in the meson propagators.

For spherically symmetric nuclei the calculation of the binding-energy shifts simplifies considerably. In this limit the eigenstates of the Dirac equation can be classified according to a generalized angular momentum κ and can be written in a two component representation; i.e.,

$$\mathcal{U}_\alpha(\mathbf{x}) \equiv \mathcal{U}_{n\kappa m}(\mathbf{x}) = \frac{1}{x} \begin{bmatrix} g_a(x) \mathcal{Y}_{+\kappa m}(\hat{\mathbf{x}}) \\ i f_a(x) \mathcal{Y}_{-\kappa m}(\hat{\mathbf{x}}) \end{bmatrix} \ ; \quad \Big(\alpha \equiv (a;m) = (n,\kappa;m)\Big) \ . \tag{17}$$

The upper and lower components are expressed in terms of spin-spherical harmonics defined by

$$\mathcal{Y}_{\kappa m}(\hat{\mathbf{x}}) \equiv \langle \hat{\mathbf{x}} | l \tfrac{1}{2} j m \rangle \ ; \quad j = |\kappa| - \frac{1}{2} \ ; \quad l = \begin{cases} \kappa \ , & \text{if } \kappa > 0; \\ -1-\kappa \ , & \text{if } \kappa < 0. \end{cases} \tag{18}$$

The binding-energy shifts can now be easily evaluated. That is,

$$\Delta E_\alpha^H = +\frac{2}{\pi^2}\int q^2 dq V_{\rm CSB}^{\rho\omega}(q)\mathcal{F}_{aH}^{(0)}(q)\ , \tag{19a}$$

$$\Delta E_\alpha^F = -\frac{2}{\pi^2}\int q^2 dq V_{\rm CSB}^{\rho\omega}(q)\mathcal{F}_{aF}^{(0)}(q)\ , \tag{19b}$$

where $q \equiv |\mathbf{q}|$ and we have defined the following quantities

$$\mathcal{F}_{aH}^{(0)}(q) \equiv \sum_b^{\rm occ}(2j_b+1)\rho_{bb0}^{(0)}(q)\rho_{aa0}^{(0)}(q)\ , \tag{20a}$$

$$\mathcal{F}_{aF}^{(0)}(q) \equiv \sum_{b;L}^{\rm occ}(2j_b+1)\Big[\langle j_a,-1/2;j_b,+1/2|L,0\rangle\rho_{abL}^{(0)}(q)\Big]^2\ . \tag{20b}$$

Note that the Fourier transform of the off-diagonal timelike-vector density has become

$$\rho_{abL}^{(0)}(q) = \int_0^\infty dx\Big[g_a(x)g_b(x)+f_a(x)f_b(x)\Big]j_L(qx)\ ;\quad (l_a+l_b+L=\text{even})\ . \tag{21}$$

Using the Bonn B potential parameters of Table I [27] we obtained the binding-energy differences reported in Table III. These values are in qualitative agreement with those reported by Blunden and Iqbal [19] and, more recently, by Barreiro, Galeão, and Krein [25]. It is interesting to note that, in contrast to the long-range Coulomb potential, the Fock term generates a substantial exchange "correction" (of the order of 30-40%) to the direct Hartree contribution. Table III also includes the remaining discrepancy between experiment and three theoretical calculations of the Coulomb displacement energy [26,43]. Note that the reported nonrelativistic discrepancies ($\Delta_{\rm DME}$ and $\Delta_{\rm SKII}$) differ—in some cases by a large fraction—from the recent relativistic estimates ($\Delta_{\rm REL}$) of Koepf, Krein, and Barreiro [26].

B. Pseudoscalar-meson sector: pseudoscalar $NN\pi$ coupling

We shall now compute the binding-energy shifts that arise from the CSB potential given in Eq. (3) using a mean-field approximation to the Walecka model. Because of the assumed pseudoscalar vertex, parity precludes a Hartree correction to the energy [23]. Thus, we only need to evaluate the Fock term. That is,

$$\Delta E_\alpha^{(\rm PS)} = +4\sum_\beta^{\rm occ}\int\frac{d\mathbf{q}}{(2\pi)^3}V_{\rm CSB}^{(5)}(\mathbf{q})\ \Big|\rho_{\beta\alpha}^{(\rm PS)}(\mathbf{q})\Big|^2\ ; \tag{22}$$

where we have introduced the Fourier transform of the off-diagonal pseudoscalar density

$$\rho_{\beta\alpha}^{(\rm PS)}(\mathbf{q}) = \int d\mathbf{x}\,\overline{\mathcal{U}}_\beta(\mathbf{x})\gamma^5 e^{-i\mathbf{q}\cdot\mathbf{x}}\,\mathcal{U}_\alpha(\mathbf{x})\ . \tag{23}$$

As in the previous section, the calculation simplifies considerably in the limit of spherically symmetric nuclei. In this limit, we obtain a binding-energy shift given by,

$$\Delta E_\alpha^{(\rm PS)} = +\frac{2}{\pi^2}\int q^2 dq V_{\rm CSB}^{(5)}(q)\mathcal{F}_a^{(\rm PS)}(q)\ , \tag{24}$$

where

$$\mathcal{F}_a^{(\mathrm{PS})}(q) \equiv \sum_{b;L}^{\mathrm{occ}} (2j_b+1)\Big[\langle j_a, -1/2; j_b, +1/2|L,0\rangle \rho_{abL}^{(\mathrm{PS})}(q)\Big]^2 \,, \tag{25}$$

and with

$$\rho_{abL}^{(\mathrm{PS})}(q) = \int_0^\infty dx \Big[g_a(x) f_b(x) + f_a(x) g_b(x)\Big] j_L(qx) \,; \quad (l_a + l_b + L = \mathrm{odd}) \,. \tag{26}$$

Note that the pseudoscalar density is, as expected, linear in the small components of the wave functions and, thus, highly sensitive to their in-medium enhancement. Moreover, the induced energy shifts are positive definite—as suggested by the ONS anomaly—for all single-particle states.

The pseudoscalar contribution to the binding-energy difference of mirror nuclei is displayed in Table III. We have listed separately the contributions arising from isospin violation in the pion-nucleon coupling constant and from π-η mixing—with the former accounting for about 60% of the total. Note that relativistic effects induce an additional enhancement in the binding-energy differences, relative to the nonrelativistic estimates of Blunden and Iqbal [19]. From Table III one observes that the binding-energy differences from the pseudoscalar sector are comparable—if not larger—than those computed originally with ρ-ω mixing. Indeed, the pseudoscalar sector—alone—accounts for about 70-85% of the discrepancy between the nonrelativistic theory and experiment.

To gauge the importance of relativity we have also computed the binding-energy differences by assuming that the lower component of the wave function is determined from the free-space relation; the upper component remained unchanged, apart from a small normalization correction. These "nonrelativistic" values appear in parenthesis in Table IV next to the uncorrected numbers. The relativistic corrections are, indeed, very significant. This is in sharp contrast to the relativistic enhancements—of less than 5%—observed for ρ-ω mixing; recall that only the dominant vector-vector component has been included, which is relatively insensitive to the enhancement of the small components of the wave function. Perhaps the result that best captures the essence of the present analysis is the ^{39}Ca-^{39}K binding-energy difference (the $1d_{3/2}^{-1}$ state in Table IV). Our baseline value for this difference is 65 keV; this represents our best attempt at reproducing the result by Blunden and Iqbal [19], namely, a nonrelativistic calculation with $g_0^\pi \equiv 0$. However, introducing, both, relativistic corrections and isospin violation in the pion-nucleon coupling constant increases the baseline value to 435 keV; this represents an enhancement of more than a factor of six.

C. Pseudoscalar-meson sector: pseudovector $NN\pi$ coupling

The above results suggest a large contribution from the pseudoscalar sector to the ONS anomaly. Yet, a definite statement awaits, as these results could be sensitive to off-shell extrapolations. Off-shell ambiguities arise from the fact that different Lorentz structures for the NN–pseudoscalar-meson vertex—which are all equivalent on-shell—can generate vastly different predictions once the nucleon is off its mass shell. Indeed, a pseudoscalar (γ^5) vertex is very sensitive to the in-medium enhancement of the lower components of the nucleon wave function, while a pseudovector coupling $[\gamma^5\gamma^\mu(p'-p)_\mu/2M]$ is not. In a model in which chiral

symmetry is not explicitly realized—such as the one employed here—a pseudovector $NN\pi$ coupling seems to be preferred, as it is known to incorporate the correct low-energy pion-nucleon dynamics without sensitive cancellations [44]. In contrast, a recent analysis of eta photoproduction data from the nucleon seems to favor a pseudoscalar $NN\eta$ coupling [31].

In this section we adopt a pseudovector representation for both ($NN\pi$ and $NN\eta$) vertices. The advantage of such a choice is that it provides us with a lower bound for the binding-energy differences of mirror nuclei within the pseudoscalar sector. This, combined with the upper bound set by the pseudoscalar representation, should adequately reflect the sensitivity of our results to the various off-shell extrapolations.

For the pseudovector case the angular-momentum algebra becomes slightly more complicated than before due to the explicit spin dependence of the operator. Recall that in the pseudoscalar case the spin dependence is implicit through the upper-to-lower coupling induced by the pseudoscalar vertex. The binding-energy shifts computed with a pseudovector $NN\pi$ coupling are now given by

$$\Delta E_{\alpha}^{(\mathrm{PV})} = +\frac{2}{\pi^2}\int q^2 dq \left(\frac{q^2}{4M^2}\right) V_{\mathrm{CSB}}^{(5)}(q)\mathcal{F}_a^{(\mathrm{PV})}(q)\ , \tag{27}$$

where

$$\mathcal{F}_a^{(\mathrm{PV})}(q) \equiv \sum_{b;J}^{\mathrm{occ}}(2j_b+1)\Big[\langle j_a,-1/2;j_b,+1/2|J,0\rangle\rho_{abJ}^{(\mathrm{PV})}(q)\Big]^2\ . \tag{28}$$

The pseudovector density has been computed in the static $[(p'-p)^0\to 0]$ limit and is given by

$$\rho_{abJ}^{(\mathrm{PV})}(q) = \sum_{L=J\pm1}\Big[C_{JL}(+\kappa_a,+\kappa_b)\int_0^\infty dx g_a(x)g_b(x)j_L(qx) + C_{JL}(-\kappa_a,-\kappa_b)\int_0^\infty dx f_a(x)f_b(x)j_L(qx)\Big]\ ;\quad (l_a+l_b+L=\mathrm{even})\ , \tag{29}$$

where

$$C_{JL}(\kappa_a,\kappa_b) \equiv \frac{(-1)^{(L+J+1)/2}}{(2J+1)}\begin{cases} L+(l_a-j_a)(2j_a+1)+(l_b-j_b)(2j_b+1)\ , & \text{if } L=J+1\ ; \\ J-(l_a-j_a)(2j_a+1)-(l_b-j_b)(2j_b+1)\ , & \text{if } L=J-1\ . \end{cases} \tag{30}$$

Note that in the static limit a pseudovector vertex does not induce an off-diagonal coupling. Hence, relativistic effects, which appear as $(f/g)^2$ corrections, are negligible. Moreover, the extra factor of q^2 that results from the pseudovector coupling is expressed in units of the free nucleon mass M—not in units of $M^\star$ (see Eq. 27). Thus, the binding-energy differences computed with a pseudovector vertex could be reproduced with a pseudoscalar vertex—only in the case in which the lower component of the wave function be determined from the free-space relation (see Table IV). Thus, the square of the effective mass in the medium relative to its free space value (i.e., $M^{\star 2}/M^2$) should serve as an indicator of the sensitivity of the approach to the various off-shell extrapolations. Note that in a mean-field approximation to the Walecka model $M^{\star 2}/M^2$ is typically of the order of 40%. Thus, off-shell ambiguities are expected to be large (see Table V).

The pseudovector contribution to the binding-energy difference of mirror nuclei is displayed, alongside the pseudoscalar results, in Table V. As suggested previously, these results are very close to those obtained in Table IV using the free upper-to-lower ratio. More significantly, however, is the very dramatic reduction in the binding-energy differences relative to the pseudoscalar results. Indeed, while a calculation with a pseudoscalar vertex accounts for about 70-85% of the ONS anomaly, only 30% of it can be explained with a pseudovector vertex. It is important to stress that although some theoretical guidelines do exist, off-shell ambiguities might be difficult to resolve given that the contribution from the isospin-violating part of the potential to hadronic observables is small.

V. CONCLUSIONS

Binding-energy differences of mirror nuclei have been computed in a model that includes two sources of charge-symmetry-breaking in the NN potential; isoscalar-isovector mixing in the meson propagator and isospin violation in the meson-nucleon coupling constants. For the vector-meson sector we have used a VMD-inspired model. Thus, on the basis of this assumption—but little else—we concluded that neither ρ-ω mixing nor the dominant vector-vector component of the vector-meson-exchange potential can contribute to the binding-energy discrepancy between theory and experiment. In models of this sort this conclusion seems unavoidable—as gauge invariance forces, both, the ρ-ω mixing amplitude and the isospin-violating vector coupling to vanish at $Q^2 = 0$. This is in contrast to previous analyses that employed the on-shell value of the ρ-ω mixing amplitude to explain the bulk of the ONS anomaly [2,19,20,21]. Hence, in our model the anomaly must be explained exclusively in terms of π-η mixing and of isospin violation in the pion-, rho-, and omega-nucleon coupling constants.

To compute the ^{3}He-^{3}H binding-energy difference a nonrelativistic estimate of the $^1S_0$ component of the CSB potential was obtained. In our model all sources of CSB generate a $^1S_0$ interaction with a long-range part that is attractive in the pp channel and repulsive in the nn channel. This result is robust, as it only depends on the sign of the π-η mixing amplitude and on the sign of the isospin-violating meson-nucleon coupling constants; recall that in our model the latter is determined from the up-down quark mass difference, which we assume to be negative. The ^{3}He-^{3}H binding-energy difference, however, was seen to be very sensitive to the short-distance behavior of the potential. Indeed, the binding-energy difference emerged from a delicate interplay between the short- and long-range parts of the potential. This interplay introduces a node in the CSB potential which can be shifted to a large enough distance as to make the binding-energy difference almost consistent with experiment. We stress that the (almost) agreement with experiment could only be achieved at the expense of introducing unrealistically soft form factors.

For the medium-mass (A=15–41) region we computed the binding-energy difference of mirror nuclei in a relativistic mean-field approximation to the Walecka model. Due to the larger size of the system, relative to ^{3}He, our results were fairly insensitive to the short-distance structure of the potential. Moreover, explicit spin-dependent effects are known to be small for these spin-saturated nuclei. As a consequence, the numerical impact from the vector-meson sector on the ONS anomaly was seen to be small. We proposed pseudoscalar-meson exchange as an alternate mechanism to explain the ONS anomaly in the medium-mass

region. We computed binding-energy differences that were comparable—and in most cases larger—than those obtained from previous estimates using on-shell ρ-ω mixing. We have concluded that the pseudoscalar sector—alone—could explain about 70-85% of the ONS anomaly. Two effects, ignored until now, were responsible for these findings: a) the inclusion of isospin violation in the pion-nucleon coupling constant, and b) relativity, which enhances the small components of the bound-state wave functions relative to their free-space value. We reached these conclusions by assuming a pseudoscalar coupling for, both, the $NN\pi$ and $NN\eta$ vertices. Yet other choices—all of them equivalent on-shell—are possible; such as pseudovector coupling. There is no definite prescription on how to take the CSB potential off-shell. Moreover, this issue is complicated further by the fact that chiral symmetry favors a pseudovector representation for the $NN\pi$ vertex while a recent analysis of η-photoproduction data seems to suggest a pseudoscalar $NN\eta$ coupling. Hence, to gauge the sensitivity of our results to the various off-shell extrapolations we repeated the calculation by adopting a pseudovector representation for both vertices. We concluded that the off-shell ambiguities were large; while 70-85% of the anomaly could be explained with a pseudoscalar coupling only 30% of it could be accounted for with a pseudovector vertex.

In conclusion, we have used a VMD-inspired model to examine the effect of isospin-violating meson-nucleon coupling constants and of π-η mixing on the binding-energy difference of mirror nuclei. We could account for most of the ^{3}He-^{3}H binding-energy difference—provided very soft form factors were assumed. Moreover, we could explain the ONS anomaly in the medium-mass region—provided a pseudoscalar representation was adopted. Based on these findings we expect that the Okamoto-Nolen-Schiffer anomaly will remain—even after more than a quarter of a century—the source of considerable theoretical debate.

ACKNOWLEDGMENTS

We thank S. Gardner, C.J. Horowitz, D. Robson, and B.D. Serot for many helpful conversations. We acknowledge the generosity of E. Pace for providing us with the three-body wave function. This work was supported by the DOE under Contracts Nos. DE-FC05-85ER250000, DE-FG05-92ER40750 and DE-FG05-86ER40273.

REFERENCES

[1] E.M. Henley and G.A. Miller, in *Mesons in Nuclei*, eds. M. Rho and D.H. Wilkinson (North-Holland, Amsterdam 1979).
[2] G.A. Miller, B.M.K. Nefkens, and I. Šlaus, Phys. Rep. **194** (1990) 1.
[3] T. Goldman, J.A. Henderson, and A.W. Thomas, *Few-Body Systems* **12** (1992) 123; Mod. Phys. Lett. **A7** (1992) 3037.
[4] J. Piekarewicz and A.G. Williams, Phys. Rev. C **47** (1993) R2462.
[5] G. Krein, A.W. Thomas, and A.G. Williams, Phys. Lett. B **317** (1993) 293.
[6] T. Hatsuda, E.M. Henley, T. Meissner, and G. Krein, Phys. Rev. C **49** (1994) 452.
[7] K.L. Mitchell, P.C. Tandy, C.D. Roberts, and R.T. Cahill, Phys. Lett. B **335** (1994) 282.
[8] H.B. O'Connell, B.C. Pearce, A.W. Thomas, and A.G. Williams, Phys. Lett. B **336** (1994) 1.
[9] K. Maltman, University of Adelaide preprint ADP-95-20/T179 and hep-ph/9504237.
[10] G.A. Miller, Chin. J. Phys. **32** (1994) 1075; G.A. Miller and W.T.H. van Oers nucl-th/9409013.
[11] H.B. O'Connell, B.C. Pearce, A.W. Thomas, and A.G. Williams, University of Adelaide preprint ADP-95-15/T176 and hep-ph/9503332.
[12] S. Gardner, C.J. Horowitz, and J. Piekarewicz, Phys. Rev. Lett. **75** (1995) 2462; Phys. Rev. C **53** (1996) 1143.
[13] J. Piekarewicz, Phys. Lett. B **358** (1995) 27.
[14] W.R. Gibbs, Li Ai, and W.B. Kaufmann, Phys. Rev. Lett. **74** (1995) 3740.
[15] L.D. Knutson *et al.,* Nucl. Phys. **A508** (1990) 185c; Phys. Rev. Lett. **66** (1991) 1410; S.E. Vigdor *et al.,* Phys. Rev. C **46** (1992) 410.
[16] I. Šlaus, Y. Akaishi, and H. Tanaka, Phys. Rep. **173** (1989) 257.
[17] K. Okamoto, Phys. Lett. **11** (1964) 150; K. Okamoto and C. Pask, Ann. of Phys. **68** (1971) 18.
[18] J.A. Nolen Jr. and J.P Schiffer, Ann. Rev. Nucl. Sci. 19 (1969) 471.
[19] P.G. Blunden and M.J. Iqbal, Phys. Lett. B **198** (1987) 14.
[20] S. A. Coon and R. C. Barrett, Phys. Rev. C **36** (1987) 2189.
[21] Y.W. Ishikawa, and T. Sasakawa, Phys. Rev. Lett. **64** (1990) 1875; Errata Phys. Rev. Lett. **66** (1991) 242.
[22] P. Numberg, D. Prosperi and E. Pace, Nucl. Phys. **A285** (1977) 58.
[23] J.D. Walecka, Ann. of Phys. **83** (1974) 491; B.D. Serot and J.D. Walecka, Adv. in Nucl. Phys. **16**, J.W. Negele and E. Vogt, eds. (Plenum, N.Y. 1986).
[24] Y. Nedjadi and J.R. Rook, Nucl. Phys. **A484** (1988) 525.
[25] L.A. Barreiro, A.P. Galeão, and G. Krein, Phys. Lett. B **358** (1995) 7.
[26] W. Koepf, G. Krein, and L.A. Barreiro, nucl-th/9601027.
[27] R. Machleidt, in *Advances in Nuclear Physics*, v. 19, eds. J.W. Negele and E. Vogt (Plenum, New York, 1989).
[28] V. Dmitrašinović and S.J. Pollock, Phys. Rev. C **52** (1995) 1061.
[29] Kim Maltman, Phys. Lett. B **362** (1995) 11.
[30] Sidney A. Coon and Michael D. Scadron, Phys. Rev. C **26** (1982) 562.
[31] L. Tiator, C. Bennhold, and S.S. Kamalov, nucl-th/9404013.
[32] J. Piekarewicz, Phys. Rev. C **48** (1993) 1555.

[33] J.L. Friar, Nucl. Phys. **A156** (1970) 43; M. Fabre de la Ripelle, Fizika **4** (1972) 1; R.A. Brandeburg, S.A. Conn, and P.U. Sauer, Nucl. Phys. **A294** (1978) 305; J.L. Friar and B.F. Gibson, Phys. Rev. C **18** (1978) 908.
[34] R.V. Reid, Ann. Phys. **50** (1968) 411.
[35] C. Ciofi degli Atti, E. Pace, and G. Salmè, Studies in High Energy Physics, vol. 2, Horwood Academic Publishers, 1979, 369; E. Pace, Lett. Nuovo Cimento **26** (1979) 615; C. Ciofi degli Atti, E. Pace, and G. Salmè, Nucl. Phys. **A358** (1981) 183c.
[36] Peter C. McNamee, Michael D. Scadron, and Sidney A. Coon, Nucl. Phys. **A249** (1975) 483.
[37] D. B. Lichtenberg, Phys. Rev. D **40** (1989) 3675.
[38] E.M. Henley and T. Meissner, nucl-th/9601030.
[39] L. Frankfurt, L. Mankiewicz, M.I. Strikman, Z. Phys. **A334** (1989) 343.
[40] S. Kumano, Phys. Rev. D **43** (1991) 59.
[41] A. Signal, A.W. Schreiber, and A.W. Thomas, Mod. Phys. Lett. **A6** (1991) 271.
[42] K. Holinde and A.W. Thomas, Phys. Rev. C **42** (1990) R1195.
[43] Hiroshi Sato, Nucl. Phys. **A269** (1976) 378.
[44] T. Matsui and B.D. Serot, Ann. Phys. **144** (1982) 107.

FIGURES

FIG. 1. The integrand for the ^{3}He-^{3}H binding-energy difference arising from one-pion exchange for three different choices of form factors: $\Lambda_{NN\pi} \to \infty$ (solid line), $\Lambda_{NN\pi} = 1.7$ GeV (dashed line) $\Lambda_{NN\pi} = 0.8$ GeV (dot-dashed line). The one-pion exchange contribution to ΔE, which is the area under the appropriate curve, appears in parentheses next to its label.

FIG. 2. The integrand for the ^{3}He-^{3}H binding-energy difference arising from one-omega exchange for three different choices of form factors: $\Lambda_{NN\omega} \to \infty$ (solid line), $\Lambda_{NN\omega} = 1.85$ GeV (dashed line) $\Lambda_{NN\omega} = 1.3$ GeV (dot-dashed line). The one-omega exchange contribution to ΔE, which is the area under the appropriate curve, appears in parentheses next to its label.

TABLES

TABLE I. Meson masses, coupling constants, tensor-to-vector ratio, and cutoff parameters of the Bonn B potential.

Meson	Mass (MeV)	$g^2/4\pi$	f/g	Λ (MeV)
π	138	14.21	—	1700
η	549	0.90	—	1700
ρ	769	0.42	6.1	1850
ω	783	11.13	0.0	1850

TABLE II. Contribution to the ^{3}He-^{3}H binding-energy difference (in keV) arising from π-η mixing, $\pi-$, $\rho-$, and $\omega-$meson exchange for three different values of the cutoff parameters; see text for details. The experimental value is $\Delta E = 71 \pm 19 \pm 5$ keV. For comparison, we also include the contribution from on-shell ρ-ω mixing.

	Point coupling	Hard form factors	Soft form factors
π-η	+7.4	+13.6	+22.2
π	−27.9	−16.2	+13.0
ρ	−49.4	−37.3	−20.4
ω	−53.8	−40.9	−22.4
Total	−123.7	−80.8	−7.6
ρ-ω	+57.9	+77.9	+87.3

TABLE III. Contribution to the binding-energy differences of mirror nuclei (in keV) arising from isospin violation in the pion-nucleon coupling constant, π-η mixing, their sum, and on-shell ρ-ω mixing. Also included are the remaining differences (Δ) between experiment and the Coulomb energy computed in three different models [26,43].

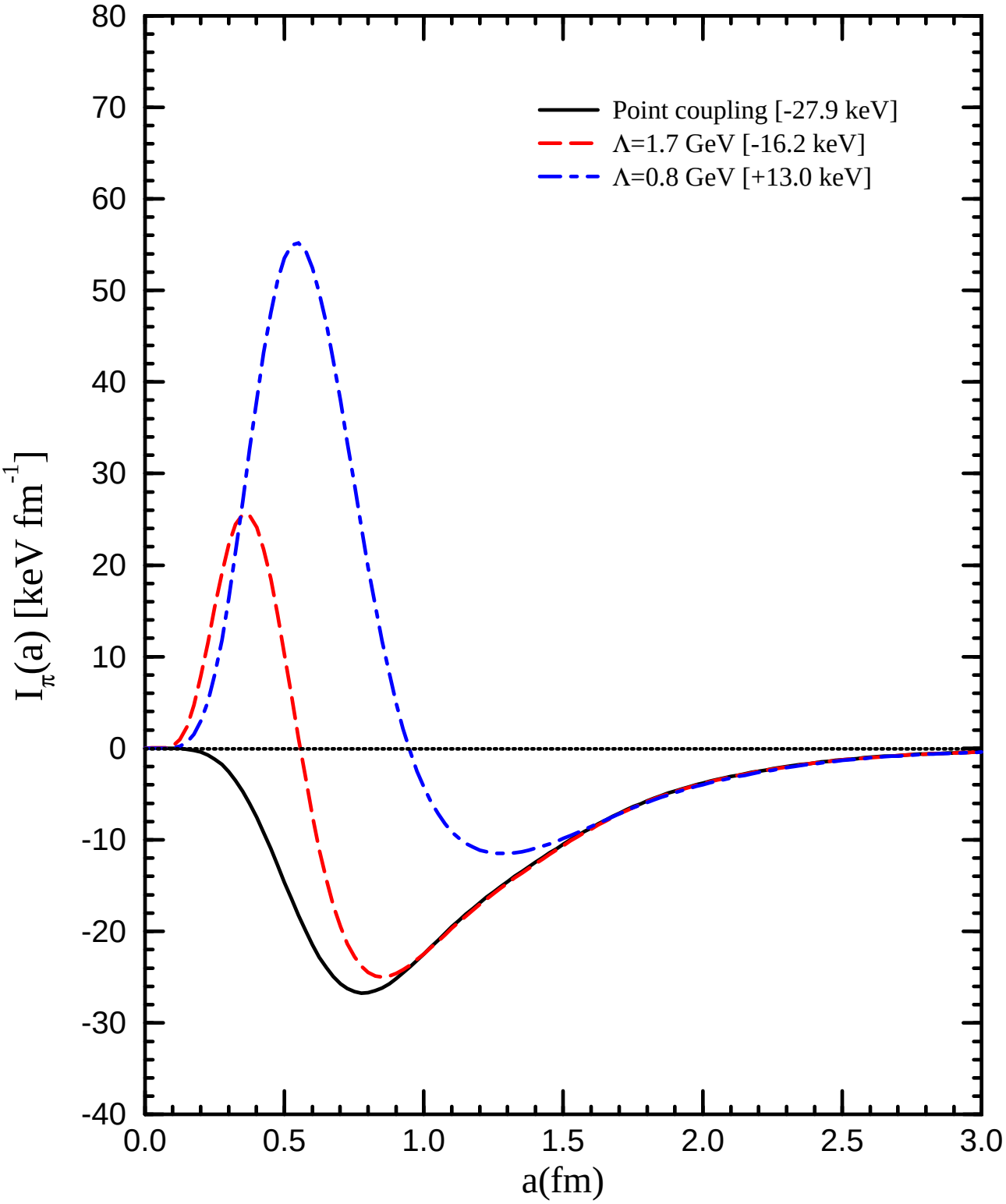
		Pseudoscalar			Rho-omega			ONS Anomaly		
A	State	$\delta g_{NN\pi}$	π-η	Total	Hartree	Fock	Total	$\Delta_{\rm DME}$	$\Delta_{\rm SKII}$	$\Delta_{\rm REL}$
15	$1p_{1/2}^{-1}$	201	145	346	379	−149	230	380	290	95
17	$1d_{5/2}$	83	56	139	246	−91	155	300	190	79
27	$1d_{5/2}^{-1}$	223	148	371	445	−176	269	480	490	551
29	$2s_{1/2}$	165	108	273	305	−91	214	290	240	34
31	$2s_{1/2}^{-1}$	202	134	336	355	−119	236	540	560	39
33	$1d_{3/2}$	159	113	272	363	−121	242	360	280	213
39	$1d_{3/2}^{-1}$	255	180	435	455	−169	286	540	430	404
41	$1f_{7/2}$	133	89	222	355	−129	226	440	350	404

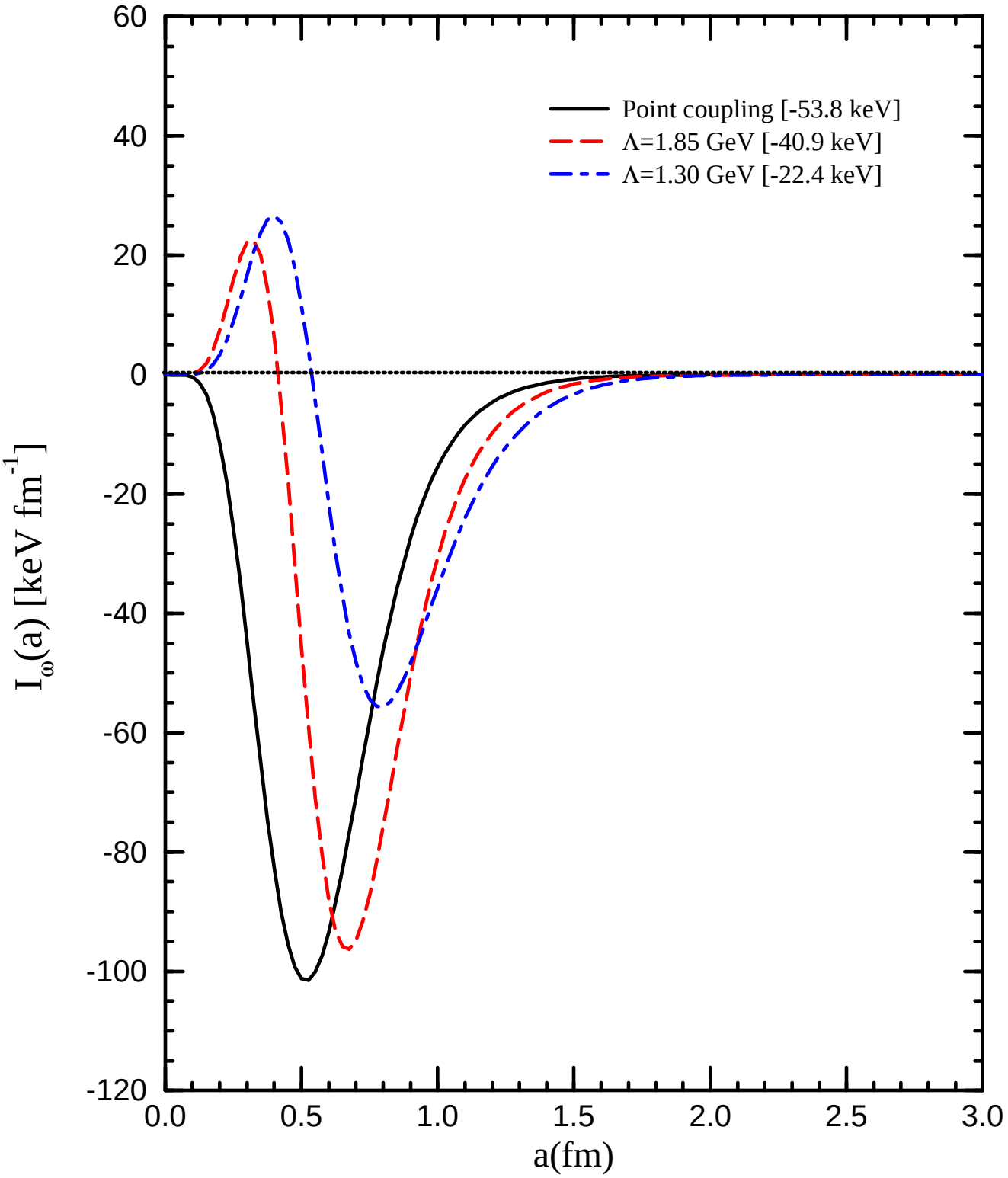
TABLE IV. Contribution to the binding-energy differences of mirror nuclei (in keV) arising from isospin violation in the pion-nucleon coupling constant, π-η mixing, their sum, and on-shell ρ-ω mixing. Included in parenthesis are the corresponding quantities computed with lower components generated from the free-space relation.

A	State	$\delta g_{NN\pi}$	π-η	Total	Rho-omega
39	$1d_{5/2}^{-1}$	205 (103)	142 (73)	347 (176)	294 (291)
	$2s_{1/2}^{-1}$	233 (84)	158 (58)	391 (142)	283 (271)
	$1d_{3/2}^{-1}$	255 (92)	180 (65)	435 (157)	286 (275)
41	$1f_{7/2}$	133 (78)	89 (53)	222 (131)	226 (224)

TABLE V. Contribution to the binding-energy differences of mirror nuclei (in keV) arising from isospin violation in the pion-nucleon coupling constant, π-η mixing, and their sum. The first(second) set of numbers were computed using a pseudoscalar(pseudovector) $NN\pi$ vertex.

		Pseudoscalar			Pseudovector		
A	State	$\delta g_{NN\pi}$	π-η	Total	$\delta g_{NN\pi}$	π-η	Total
15	$1p_{1/2}^{-1}$	201	145	346	67	49	116
17	$1d_{5/2}$	83	56	139	52	36	88
27	$1d_{5/2}^{-1}$	223	148	371	109	74	183
29	$2s_{1/2}$	165	108	273	54	36	90
31	$2s_{1/2}^{-1}$	202	134	336	62	43	105
33	$1d_{3/2}$	159	113	272	49	35	84
39	$1d_{3/2}^{-1}$	255	180	435	83	59	142
41	$1f_{7/2}$	133	89	222	74	51	125


Point coupling [-27.9 keV]
Λ=1.7 GeV [-16.2 keV]
Λ=0.8 GeV [+13.0 keV]
I_π(a) [keV fm^-1]
a(fm)
80
70
60
50
40
30
20
10
0
-10
-20
-30
-40
0.0
0.5
1.0
1.5
2.0
2.5
3.0


Point coupling [-53.8 keV]
Λ=1.85 GeV [-40.9 keV]
Λ=1.30 GeV [-22.4 keV]
60
40
20
0
-20
-40
-60
-80
-100
-120
0.0
0.5
1.0
1.5
2.0
2.5
3.0
a(fm)
I_ω(a) [keV fm^-1]